Triboelectric Nanogenerator for Harvesting Wind Energy and as Self-Powered Wind Vector Sensor System

Ya Yang,[†,§] Guang Zhu,[†,§] Hulin Zhang,[†] Jun Chen,[†] Xiandai Zhong,[‡] Zong-Hong Lin,[†] Yuanjie Su,[†] Peng Bai,[†] Xiaonan Wen,[†] and Zhong Lin Wang[†,‡,*]

[†]School of Materials Science and Engineering, Georgia Institute of Technology, Atlanta, Georgia 30332-0245, United States and [‡]Beijing Institute of Nanoenergy and Nanosystems, Chinese Academy of Sciences, Beijing 100085, China. [§]Y. Yang and G. Zhu contributed equally to the work.

ABSTRACT We report a triboelectric nanogenerator (TENG) that plays dual roles as a sustainable power source by harvesting wind energy and as a self-powered wind vector sensor system for wind speed and direction detection. By utilizing the wind-induced resonance vibration of a fluorinated ethylene–propylene film between two aluminum foils, the integrated TENGs with dimensions of 2.5 cm × 2.5 cm × 22 cm deliver an output voltage up to 100 V, an output current of 1.6 μA, and a corresponding output power of 0.16 mW under an external load of 100 MΩ, which can be used to directly light up tens of commercial light-emitting diodes. Furthermore, a self-powered wind vector sensor system has been developed based on the rationally designed TENGs, which is capable of detecting the wind direction and speed with a sensitivity of 0.09 μA/(m/s). This work greatly expands the applicability of TENGs as power sources for self-sustained electronics and also self-powered sensor systems for ambient wind detection.

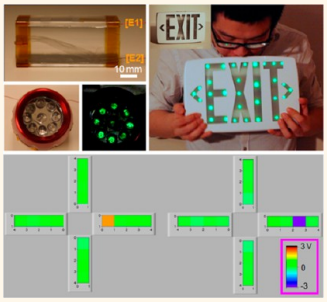

KEYWORDS: triboelectric nanogenerator · wind energy · self-powered · vector sensor · wind sensor

As one of the most important renewable and green energy sources in nature, wind energy has attracted increasing attention in the past decade due to the threat of global warming and the energy crisis.[1−3] Based on electromagnetic and piezoelectric mechanisms, conventional approaches of wind energy harvesting have been developed.[4−6] The main drawbacks of these wind energy harvesters are the complex structure, the large volume, and the mechanical wear induced performance degradation. Owning to the coupling between triboelectrification and electrostatic induction, triboelectric nanogenerators (TENGs), as an innovative invention, recently have been widely utilized to effectively scavenge mechanical energy from impacts,[7−9] sliding,[10,11] and rotations.[12] These reported TENGs exhibit the remarkable characteristics of easy fabrication, low cost, and high efficiency. In this regard, developing TENG technology to harvest wind energy is of great necessity, which will not only decrease the cost of wind energy harvesting but also greatly extend the potential applications of TENGs.

Usually, a wind vector sensor system functions for wind speed and direction, which plays a critical role in weather forecasting. The working mechanisms of the designed wind sensors include mechanical rotation,[13] temperature change,[14] and laser Doppler.[15] These sensors need to run on external power sources or conventional batteries, which will limit their applications in remote areas to collect wind information in real time. One creative approach to resolve the power limitation issue is to build up a self-powered system that operates independently, sustainably, and wirelessly by itself without using a battery.[16−18] TENGs have been utilized as self-powered sensors for detecting displacement, mercury ions/catechin, and the change of magnetic field.[11,19−21]

In this paper, we report a triboelectric effect based wind energy harvester as a sustainable power source and a self-powered wind vector sensor system for wind speed and direction detection. The as-fabricated wind energy harvester is based on periodic contact/separation between two aluminum (Al) foils and a fluorinated ethylene–propylene (FEP) film with a surface of nanowire

* Address correspondence to zlwang@gatech.edu.

Received for review August 18, 2013 and accepted September 13, 2013.

Published online September 17, 2013
10.1021/nn4043157

structures. By utilizing the coupling between the triboelectric effect and the electrostatic effect, the periodic change of distance between the two Al foils and the FEP film can induce charge transfer between the Al electrode and the ground, resulting in the flow of free electrons in the external circuit as an alternating current. The integrated TENGs with a size of 2.5 cm × 2.5 cm × 22 cm deliver an output voltage up to 100 V and an output current of 1.6 μA, which can be used to directly drive tens of commercial light-emitting diodes (LEDs). Furthermore, relying on the wind flow induced current and voltage output, a self-powered wind vector sensor system has been developed to detect the wind speed and direction. This work is important progress toward the practical applications of wind energy harvesting and the related self-powered sensor systems.

RESULTS AND DISCUSSION

The fabricated TENG consists of two Al foils and a FEP film in a cuboid acrylic tube, as schematically illustrated in Figure 1a. The Al foil plays dual roles as a triboelectric

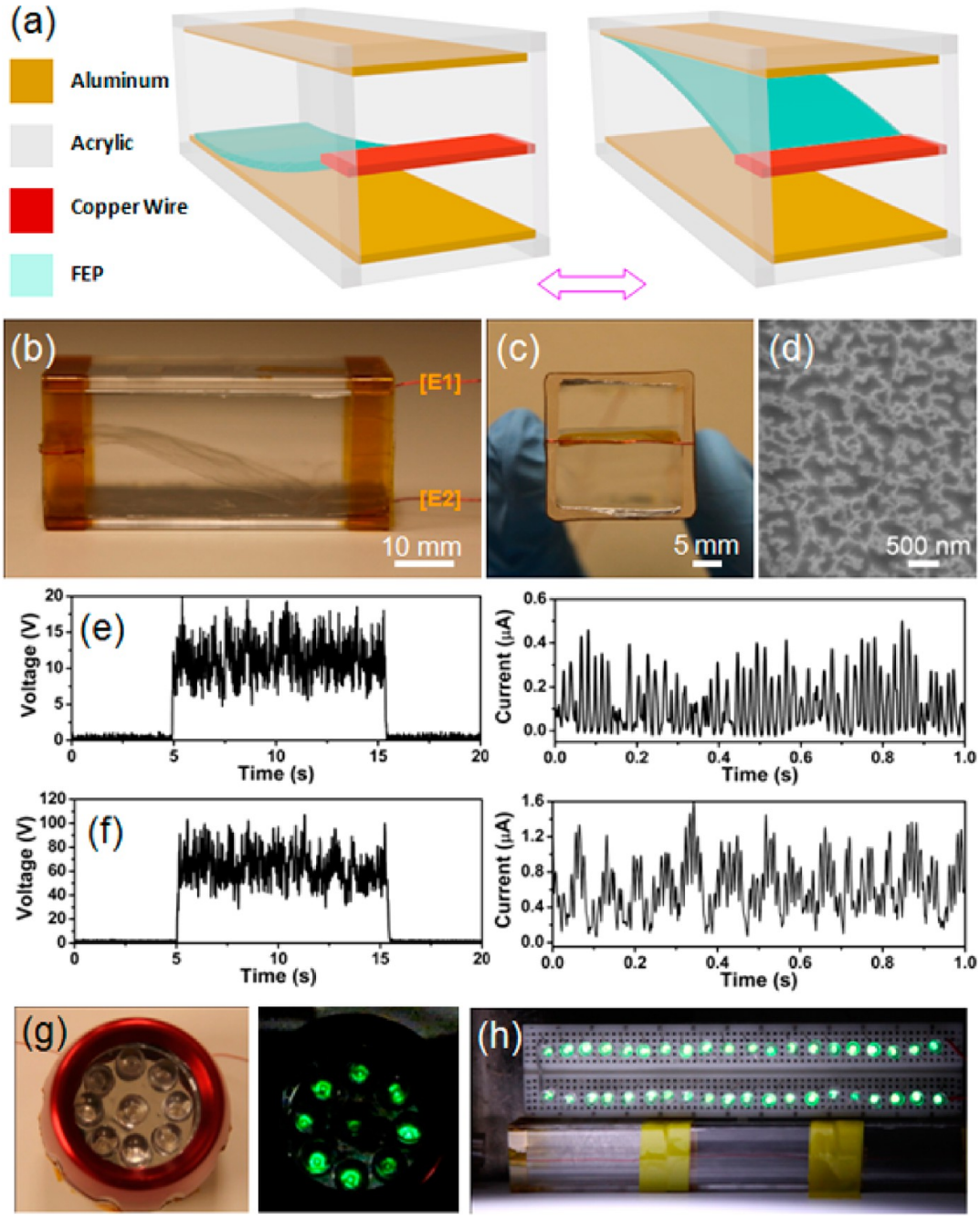

Figure 1. (a) Schematic diagram of the TENG. (b, c) Photographs of the TENG. (d) SEM image of the etched FEP film surface. (e, f) Rectified output voltage and current of one (e) and four (f) TENGs under a loading resistance of 100 MΩ. (g) Photographs of a 9-LED flashlight before and after being driven. (h) Photograph of the 40 green LEDs driven by the integrated TENGs.

surface and as an electrode. One side of the FEP film was fixed at the middle of the end surface of the tube, leaving the other side free-standing. The distance between the two Al foils and the FEP film can be changed periodically due to the wind-induced vibration of the FEP film, resulting in an output voltage/current across an external loading resistor. Figure 1b and c are the side view and front view of a typical as-fabricated TENG, indicating that the device has the dimensions 2.5 cm × 2.5 cm × 5.5 cm. The device electrode E1 or E2 is connected with an external loading resistance of 100 MΩ to the ground. To increase the triboelectric charge density, FEP nanowires are created on the surface of the FEP film *via* an inductively coupled plasma method, as shown in Figure 1d.

To investigate the TENG's performance for harvesting wind energy, an air gun that provides uniform air flow was employed as a wind source with tunable flow speed. Figure S1 depicts the measured output voltage and current of the fabricated TENG under a wind speed of about 10 m/s, where the voltage and current are about 5 V and 0.5 μA under a loading resistance of 100 MΩ, respectively. Figure 1e presents the rectified output voltage and current of the TENG. The rectified output current of the TENG is still about 0.5 μA, while the output voltage can be increased to about 20 V, which is associated with the parasitic capacitance in the bridge rectification circuit under the high working frequency and the large loading resistance. Due to the charging effect of the parasitic capacitance, the output voltage of the TENG can be increased in this study. To increase the output power of the device, four TENGs were integrated in one acrylic tube, as illustrated in Figure S2. The top and bottom Al electrodes were connected with two bridge rectification circuits, respectively. Then the two bridge rectification circuits were connected in parallel. The measured output voltage and current of the integrated TENGs can be increased to 100 V and 1.6 μA, respectively, corresponding to an output power of 0.16 mW. The increase of the total output is due to the increase of the current flow through the external loading resistor. The output signals of the TENGs were rectified and then were connected in parallel. The total output performance can be enhanced further by connecting more TENG units. To demonstrate that the produced energy can be utilized as an effective power source, one TENG with a size of 2.5 cm × 2.5 cm × 5.5 cm was fixed on a car, as displayed in Figure S3. The device was then connected with a bridge rectification circuit and a 9-LED flashlight. The photograph in Figure 1g indicates that the TENG can harvest the wind energy induced by the movement of a car and light up the flashlight, which can be also seen in the movie file 1 (see the Supporting Information). Figure 1h illustrates that the produced energy of the four integrated TENGs can be used to directly drive 40 green LEDs, as shown in movie file 2 (see the Supporting Information).

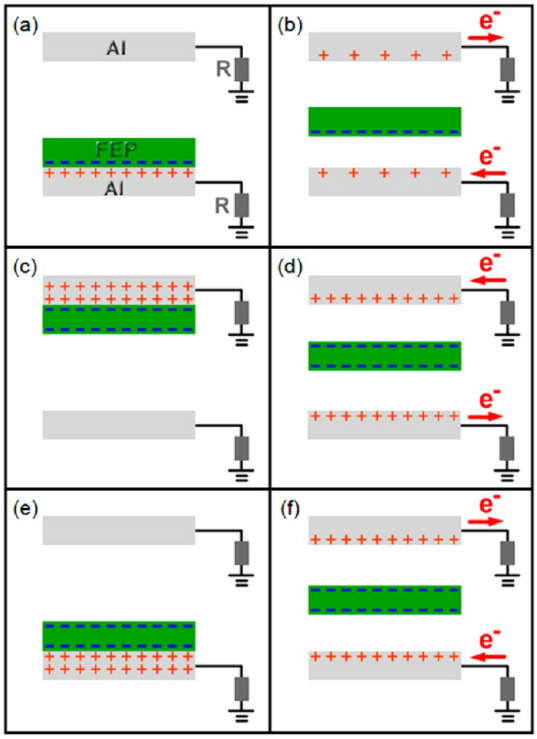

Figure 2. Sketches that illustrate the electricity generation process in a full cycle under the wind-induced vibration of the FEP film between two Al foils.

A cycle of electricity generation of the fabricated TENG is illustrated in Figure 2. At the initial state, the surfaces of the bottom Al foil and the FEP film fully contact each other, inducing charge transfer between them. According to the triboelectric series,[22] the electrons are injected from Al to FEP, resulting in positive and negative triboelectric charges on the Al and FEP surfaces, respectively. Figure 2a displays that the produced triboelectric charges with opposite polarities are fully balanced; no electron flow occurs in the external circuit. Once a wind flow separates the FEP film from the bottom Al, these triboelectric charges cannot be compensated. The negative ones on the FEP film will drive free electrons to flow through the external circuits, where the movement directions of electrons are opposite at the top and bottom Al electrodes, as depicted in Figure 2b. This electrostatic induction process can give the output voltage/current signals until the negative triboelectric charges on the FEP film are fully screened from the induced positive charges as well as the contact-induced triboelectric positive charges. No output voltage/current signals can be observed at this state, as illustrated in Figure 2c. When the FEP film was moved back from the top Al electrode to the bottom Al electrode, the negative triboelectric charges on the FEP film can induce the electrons to flow from the ground to the top Al electrode due to the increase of the relative separation between the top Al

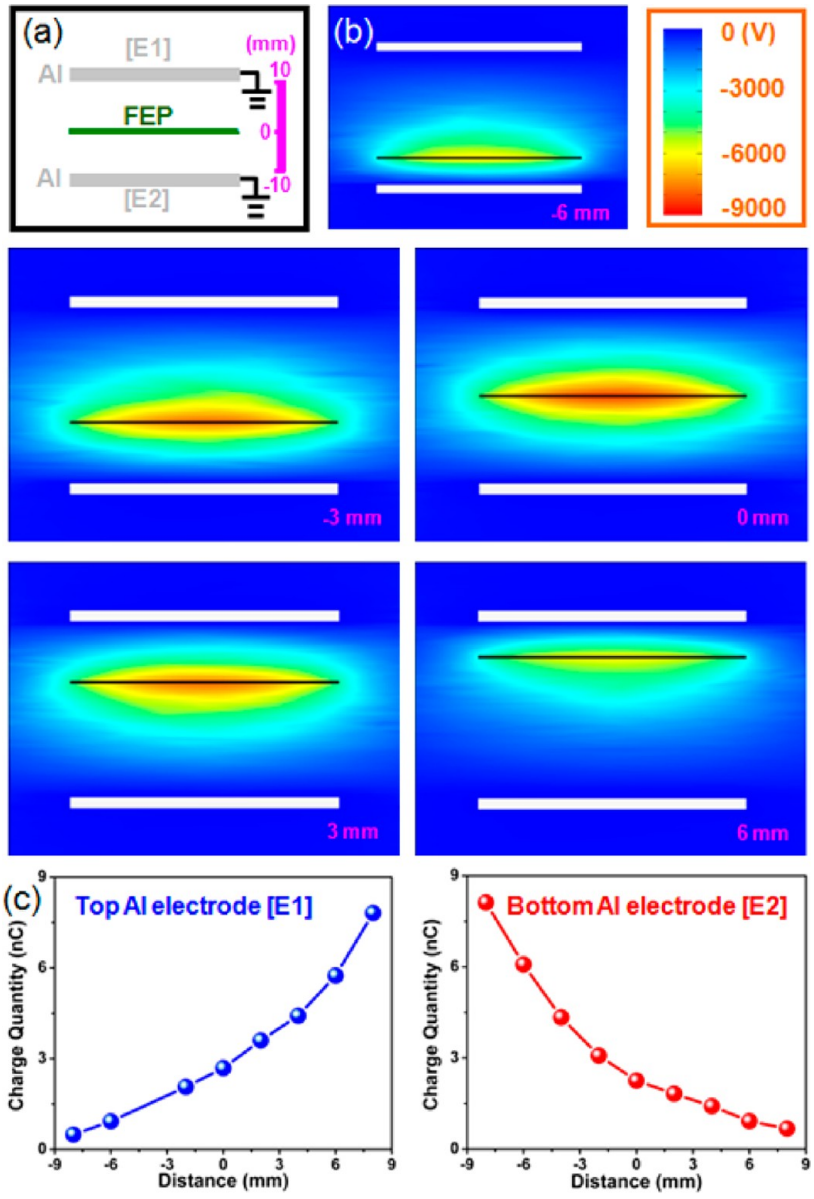

Figure 3. (a) Schematic diagram of the model for the calculation. (b) Finite-element simulation of the potential distribution in the TENG under the different positions of the FEP film between two Al electrodes. (c) Total charges on the two Al electrodes as a function of the positions of the FEP film.

electrode and the FEP film. Moreover, the electrons can be driven to flow from the bottom Al electrode to the ground due to the decrease of the distance between the FEP and the bottom Al electrode, as shown in Figure 2d. When the FEP film is in contact with the bottom Al electrode, the negative triboelectric charges on the two surfaces of the FEP film are fully screened by the induced positive charges, resulting in no electron flow in the external circuit, as shown in Figure 2e. When the FEP film was moved again from the bottom Al electrode to the top Al electrode, Figure 2f displays that the opposite voltage/current signals can be observed in the external circuit as compared with those in Figure 2d. Therefore, when the wind flow vibrates the FEP film up and down, the TENG acts as an electron pump that drives electrons back and forth between the Al electrodes and the ground, producing alternating current in the external circuit. As shown in Figure 2b, two circuits were used to connect the top and bottom Al electrodes, respectively. When the FEP film moved between the two Al electrodes, the output signals at both the top and bottom electrodes can be obtained by using the two circuits. The output signals were then rectified and connected in parallel, producing the largest electric output.

To obtain a more quantitative understanding of the proposed electricity generation mechanism of the TENG, the electric potential distribution and the charge transfer between the Al electrodes and the FEP film can be verified through finite-element simulation using

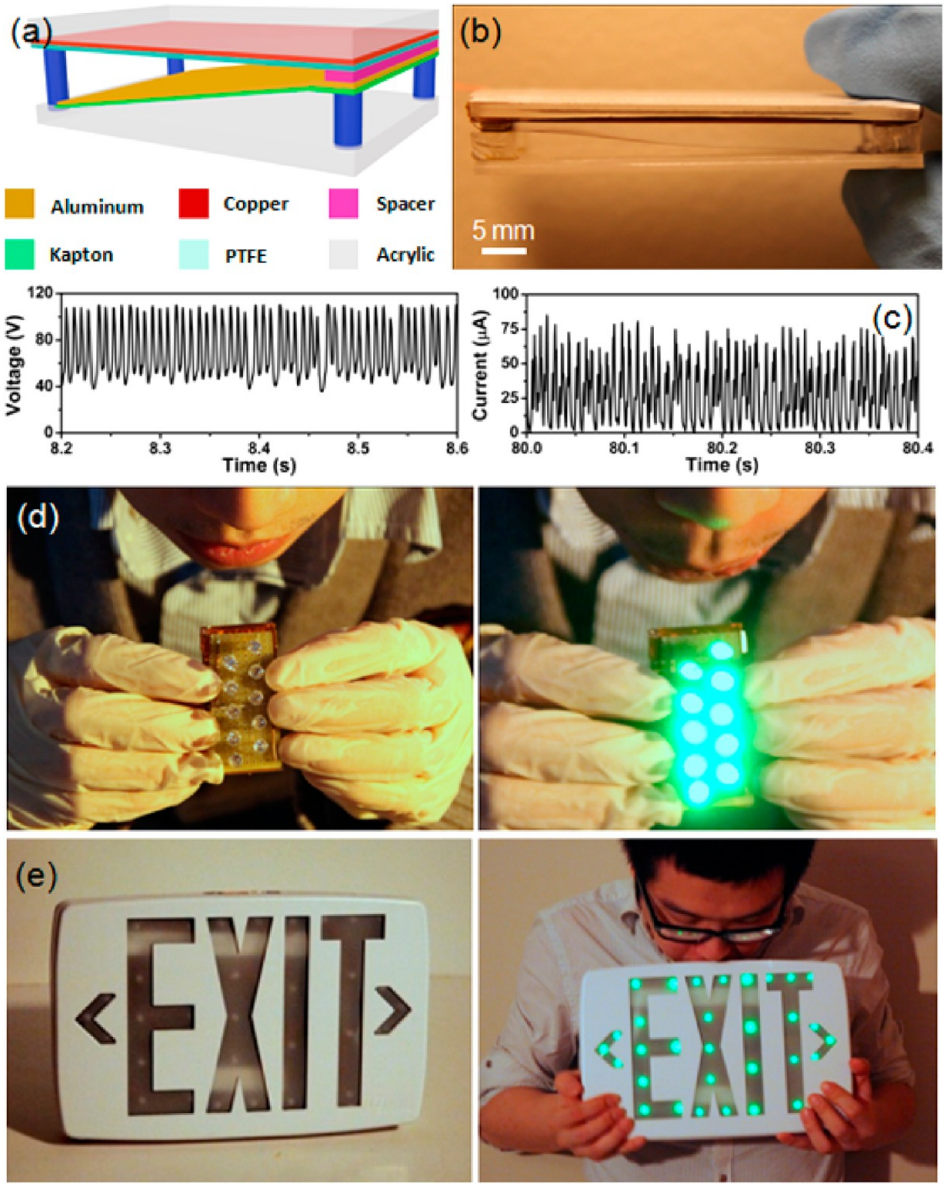

Figure 4. (a) Schematic diagram of the designed double-electrode-based TENG. (b) Photograph of the TENG. (c) Measured open-circuit voltage and the short-circuit current of the TENG under a wind speed of 10 m/s. (d, e) Photographs show that the TENG was used to harvest the human mouth blowing induced wind energy to drive 10 LEDs (d) and an exit sign (e).

COMSOL. Figure 3a illustrates a schematic diagram of the constructed model including a FEP film (20 mm × 30 mm × 25 μm) and two Al electrodes (20 mm × 30 mm × 1 mm), which were grounded. The triboelectric charge densities on the two surfaces of the FEP film were assumed to be -10 μC/m^2. Figure 3b shows the calculated results of the electric potential distribution in the TENG under the different positions at -6, -3, 0, 3, and 6 mm, respectively. When the FEP film occurs at the middle position between the two Al electrodes, it has the largest electrical potential, up to -9000 V. The electric potential on the FEP film was found to decrease dramatically when approaching the top or bottom Al electrode, as depicted in Figure 3b. Figure 3c shows the change of the total charge quantities on the Al electrodes at the different positions of the FEP film. When the FEP film departs from the bottom Al electrode to the top Al electrode, the charge quantities on the top and bottom Al electrodes increase and decrease, respectively, revealing that the opposite voltage/current signals can be obtained at the top and bottom Al electrodes.

Meanwhile, due to the diversity of contact electrification, an additional double-electrode-based TENG has also been developed for wind energy harvesting in this study. The working mechanism of the TENG is based on the contact/separation between two triboelectric material layers to drive the electrostatic induction charge flow in the external circuit.[23] Figure 4a presents a schematic diagram of the TENG, which consists of a copper electrode, a polytetrafluoroethylene (PTFE) film, and an Al electrode on a Kapton film as the

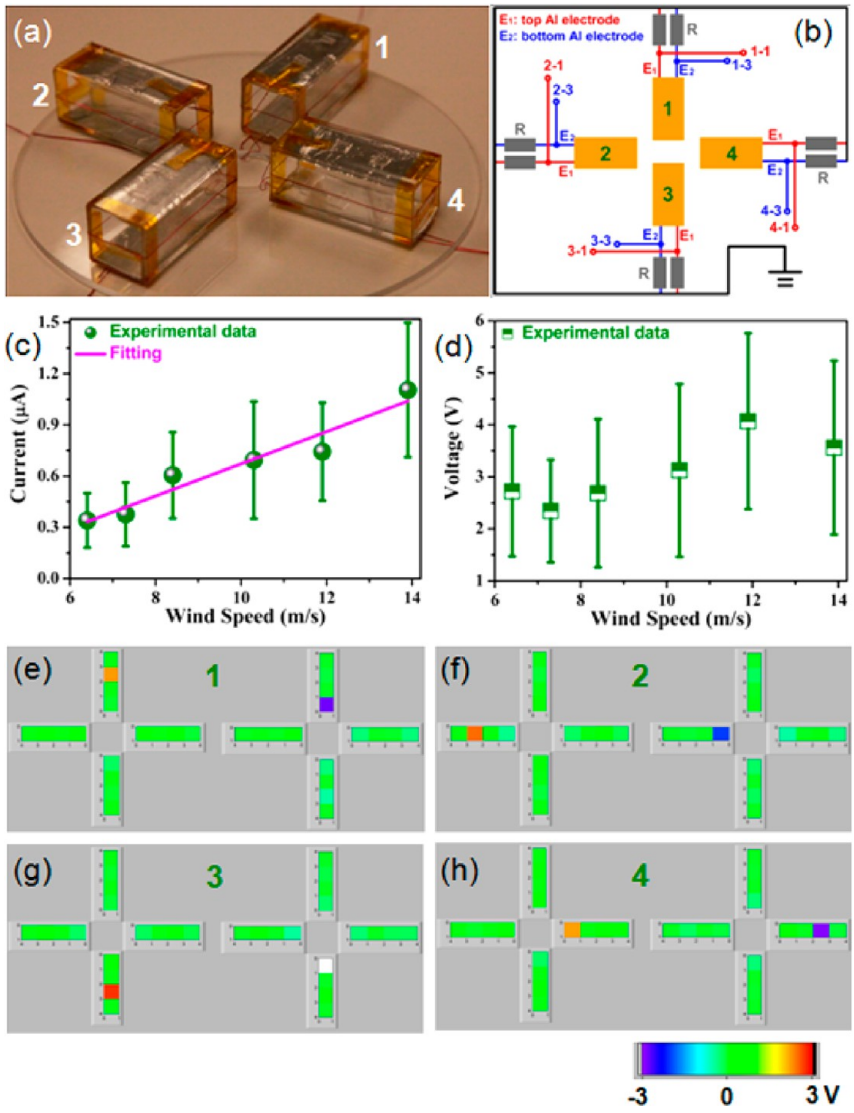

Figure 5. (a) Photograph of the four TENGs arranged along four different directions. (b) Schematic diagram of the fabricated wind vector sensor system. (c, d) Measured output current (c) and voltage (d) of one TENG under different wind speeds. (e–h) Measured output voltage mapping figures when the wind occurs along the four different directions.

wind-sensitive unit. As illustrated in Figure 4b, the photograph of the TENG indicates that the device has the dimensions 2.5 cm × 0.6 cm × 5 cm. The Al, Kapton, and the bottom acrylic can also form a single-electrode-based TENG. However, the short distance (<5 mm) between the Kapton film and the bottom acrylic can result in a much smaller output performance than that of the top double-electrode-based TENG. Thus we did not consider the bottom single-electrode-based TENG for this case. Figure S4 displays that the TENG has an open-circuit voltage up to 110 V under a wind speed of about 10 m/s. As depicted in Figure 4c, the enlarged voltage–time curve reveals that the output voltage changes between 40 and 110 V, which is associated with the high working frequency of the device. The measured largest short-circuit current of the TENG is about 80 μA. The produced electricity energy can be used to directly drive 10 LEDs by scavenging the human mouth blowing induced wind energy, as displayed in Figure 4d and movie file 3 (see the Supporting Information). An exit sign can also be driven by the produced energy, as shown in Figure 4e and movie file 4 (see the Supporting Information).

To prove the capability of the TENG as an active wind vector sensor, a set of practical applications were demonstrated for monitoring the wind speed and direction. Figure 5a displays a photograph of the sensor system, where four TENGs were arranged along four directions, respectively. Each electrode was connected with a loading resistance of 20 MΩ and then ground, as illustrated in Figure 5b. The wind speed was determined by the measured output current signals. Figure S5 depicts the measured output current and voltage signals at the bottom Al electrode along direction 1. The changes of the output current and voltage peaks with the wind speed are displayed in

Figure 5c and d, respectively. It can be clearly seen that the average output current peak dramatically increases with increasing wind speed. A linear relationship between them can be obtained by fitting the data, where the sensitivity of the wind speed is about 0.09 μA/(m/s). The output voltage peaks growingly fluctuate in a range of 1 to 6 V with increasing wind speed, and the wind direction can be determined by the analysis of the measured output voltage signals. The different changes of the current and voltage upon increasing the wind speed may be associated with the different reset times for the current and voltage.

As displayed in Figure 5b, the top and bottom electrodes of the TENG along each direction were connected with the first and third data acquisition channels, respectively. To avoid the possible noise signals, the other eight channels were grounded. The positive and negative output voltage signals in 16 channels were recorded in real time as a mapping figure. The wind direction can be attained by analysis of the measured voltage mapping figures. When no wind was applied along the four directions, there are no observed output voltage signals in the obtained mapping figure, as displayed in Figure S6a. Figure S6b shows that the measured noise signals are smaller than 0.5 V. When the wind was applied along direction 1, the obtained mapping figure in Figure 5e shows that one negative output voltage signal can be observed in the channel 1-1. The corresponding output voltage is about 2.8 V, as displayed in Figure S7. Moreover, a positive output voltage signal of about 2.3 V occurs in channel 1-3, as shown in Figure 5e and Figure S7. When the wind was applied along each direction, the recorded mapping figures clearly reveal that the output voltages in channels 1 and 3 along each direction have the opposite values, as displayed in the movie file 5 (see the Supporting Information). These results are consistent with the calculated results in Figure 3. By the analysis of the measured voltage mapping figures, the wind direction can be confirmed. As illustrated in Figure 5f–h, the three measured mapping figures clearly indicate that the wind directions are from 2, 3, and 4, respectively. These output voltage signals can also be seen in Figures S8–S10.

CONCLUSION

In summary, we have demonstrated a TENG, consisting of an FEP film and two Al foils connected with a ground through an external load. The mechanism of the TENG is based on the charge transfer between the Al electrode and the ground by utilizing the wind-induced vibration of the FEP film between the two Al electrodes. The integrated TENGs produce an output voltage up to 100 V, an output current of 1.6 μA, and an output power of 0.16 mW under a load of 100 MΩ, which can be used to light up tens of commercial LEDs. An additional double-electrode-based TENG is also demonstrated to harvest wind energy from a human blowing, and the produced electricity is enough to power an exit sign. Moreover, the TENGs have been utilized to design a self-powered wind vector sensor system for detecting the wind speed and direction. The detection sensitivity of the wind speed is about 0.09 μA/(m/s). The wind direction can be determined by the analysis of the real-time measured output voltage signals as a mapping image. This invention may push forward a significant step toward the practical applications of wind energy harvesting techniques and self-powered sensor systems.

EXPERIMENTAL SECTION

Fabrication of the TENG and the Self-Powered Wind Vector Sensor System. The fabricated TENG is based on wind-driven vibration of a FEP film between two Al foils in an acrylic tube, where each Al electrode was connected to the ground across an external load resistor. The surface of the FEP film can be dry-etched using ICP to create the nanowire structures. Specifically, O_2, Ar, and CF_4 gases with a flow ratio of 10, 15, and 30 sccm were introduced in the ICP chamber. The FEP film was etched for 15 s to produce nanowire-like structures. The double-electrode-based TENG consists of a copper film, a PTFE film, and an Al film on a Kapton film, which was used as the wind-sensitive unit. For the self-powered wind vector sensor system, four TENGs were arranged along four directions, where the top and bottom Al electrodes were connected with the data acquisition channels 1 and 3 for each direction. The other data acquisition channels were grounded. A load resistor of about 20 MΩ was connected between each Al electrode of the TENG and ground. The wind speed can be determined by the analysis of the obtained output current signals. The wind direction can be confirmed by the analysis of the measured output voltage mapping figures.

Measurement of the Fabricated Devices. In the voltage measurement process, the TENGs were connected with a low-noise voltage preamplifier (Keithley 6514 System electrometer). The output current signals of the TENGs were measured by a low-noise current preamplifier (Stanford Research SR570). For the self-powered wind vector sensor system, a homemade data acquisition system was used to record the output voltage signals in real time.

Conflict of Interest: The authors declare no competing financial interest.

Acknowledgment. This work was supported by the U.S. Department of Energy, Office of Basic Energy Sciences (DE-FG02-07ER46394), NSF, and the Knowledge Innovation Program of the Chinese Academy of Sciences (KJCX2-YW-M13). The authors thank Guang Zhu, Zong-Hong Lin, and Peng Bai for their contributions of the double-electrode-based triboelectric nanogenerators in Figure 4.

Supporting Information Available: Additional figures include the output voltage and current of the TENG at the top and bottom Al electrodes, a photograph of the four integrated TENGs in an acrylic tube, an optical image of the TENG fixed on a car, the measured open-circuit voltage of the double-electrode-based TENG, the measured output voltage and current of the TENG under the different wind speeds, the mapping figure of the measured output voltage signals and the corresponding voltage-channel curve under the condition of no wind, and the output voltage signals in the 16 channels when the wind was applied along the four directions. Additional movie files include

one TENG powering a 9-LED flashlight, integrated TENGs lighting up 40 green LEDs, the double-electrode-based TENG to harvest human mouth blowing induced wind energy for driving 10 LEDs and an exit sign, and the measured output voltage mapping figures under different wind conditions. This material is available free of charge *via* the Internet at http://pubs.acs.org.

REFERENCES AND NOTES

1. Zhou, Y.; Luckow, P.; Smith, S. J.; Clarke, L. Evaluation of Global Onshore Wind Energy Potential and Generation Costs. *Environ. Sci. Technol.* **2012**, *46*, 7857–7864.
2. Tapia, A.; Tapia, G.; Ostolaza, J. X.; Saenz, J. R. Modeling and Control of a Wind Turbine Driven Doubly Fed Induction Generator. *IEEE Trans. Energy Convers.* **2003**, *18*, 194–204.
3. Herbert, G. M. J.; Iniyan, S.; Sreevalsan, E.; Rajapandian, S. A Review of Wind Energy Technologies. *Renew. Sustainable Energy Rev.* **2007**, *11*, 1117–1145.
4. Bressers, S.; Avirovik, D.; Vernieri, C.; Regan, J.; Chappell, S.; Hotze, M.; Luhman, S.; Lallart, M.; Inman, D.; Priya, S. Small-Scale Modular Windmill. *Am. Ceram. Soc. Bull.* **2010**, *89*, 34–40.
5. Priya, S. Modeling of Electric Energy Harvesting Using Piezoelectric Windmill. *Appl. Phys. Lett.* **2005**, *87*, 184101.
6. Myers, R.; Vickers, M.; Kim, H.; Priya, S. Small Scale Windmill. *Appl. Phys. Lett.* **2007**, *90*, 054106.
7. Fan, F.-R.; Tian, Z.-Q.; Wang, Z. L. Flexible Triboelectric Generator. *Nano Energy* **2012**, *1*, 328–334.
8. Zhu, G.; Pan, C.; Guo, W.; Chen, C.-Y.; Zhou, Y.; Yu, R.; Wang, Z. L. Tiboelectric-Generator-Driven Pulse Electrodeposition for Micropatterning. *Nano Lett.* **2012**, *12*, 4960–4965.
9. Wang, S.; Long, L.; Wang, Z. L. Nanoscale Triboelectric-Effect-Enabled Energy Conversion for Sustainably Powering Portable Electronics. *Nano Lett.* **2012**, *12*, 6339–6346.
10. Zhu, G.; Chen, J.; Liu, Y.; Bai, P.; Zhou, Y.-S.; Jing, Q.-S.; Pan, C.-F.; Wang, Z. L. Linear-Grating Triboelectric Generator Based on Sliding Electrification. *Nano Lett.* **2013**, *13*, 2282–228.
11. Yang, Y.; Zhang, H.; Chen, J.; Jing, Q.; Zhou, Y. S.; Wen, X.; Wang, Z. L. Single-Electrode-Based Sliding Triboelectric Nanogenerator for Self-Powered Displacement Vector Sensor System. *ACS Nano* **2013**, *7*, 7342–7351.
12. Lin, L.; Wang, S.; Xie, Y.; Jing, Q.; Niu, S.; Hu, Y.; Wang, Z. L. Segmentally Structured Disk Triboelectric Nanogenerator for Harvesting Rotational Mechanical Energy. *Nano Lett.* **2013**, *13*, 2916–2923.
13. Du, L.; Zhao, Z.; Fang, Z.; Xu, J.; Geng, D.; Liu, Y. A Micro-Wind Sensor Based on Mechanical Drag and Thermal Effects. *Sensor. Actuat. A: Phys.* **2009**, *155*, 66–72.
14. Shen, G.-P.; Qin, M.; Huang, Q.-A. A Cross-Type Thermal Wind Sensor with Self-Testing Function. *IEEE Sens. J.* **2010**, *10*, 340–346.
15. Harris, M.; Constant, G.; Ward, C. Continuous-Wave Bistatic Laser Doppler Wind Sensor. *Appl. Opt.* **2001**, *40*, 1501–1506.
16. Wang, Z. L.; Wu, W. Nanotechnology-Enabled Energy Harvesting for Self-Powered Micro/Nanosystems. *Angew. Chem., Int. Ed.* **2012**, *51*, 11700–11721.
17. Xu, S.; Qin, Y.; Xu, C.; Wei, Y.; Yang, R.; Wang, Z. L. Self-Powered Nanowire Devices. *Nat. Nanotechnol.* **2010**, *5*, 366–373.
18. Hu, Y.; Zhang, Y.; Xu, C.; Lin, L.; Snyder, R. L.; Wang, Z. L. Self-Powered System with Wireless Data Transmission. *Nano Lett.* **2011**, *11*, 2572–2577.
19. Lin, Z. H.; Zhu, G.; Zhou, Y. S.; Yang, Y.; Bai, P.; Chen, J.; Wang, Z. L. A Self-Powered Triboelectric Nanosensor for Mercury Ion Detection. *Angew. Chem., Int. Ed.* **2013**, *125*, 5169–5173.
20. Lin, Z. H.; Xie, Y.; Yang, Y.; Wang, S.; Zhu, G.; Wang, Z. L. Enhanced Triboelectric Nanogenerators and Triboelectric Nanosensor Using Chemically Modified TiO_2 Nanomaterials. *ACS Nano* **2013**, *7*, 4554–4560.
21. Yang, Y.; Lin, L.; Zhang, Y.; Jing, Q.; Hou, T.-C.; Wang, Z. L. Self-Powered Magnetic Sensor Based on a Triboelectric Nanogenerator. *ACS Nano* **2012**, *6*, 10378–10383.
22. Shashoua, V. E. Static Electricity in Polymers. I. Theory and Measurement. *J. Polym. Sci.* **1958**, *33*, 65–85.
23. Yang, Y.; Zhang, H.; Chen, J.; Lee, S.; Hou, T.-C.; Wang, Z. L. Simultaneously Harvesting Mechanical and Chemical Energies by a Hybrid Cell for Self-Powered Biosensors and Personal Electronics. *Energy Environ. Sci.* **2013**, *6*, 1744–1749.